2021-02-08

# Selenite induces apoptosis in sarcomatoid malignant mesothelioma cells through oxidative stress

Nilsonne, Gustav; Sun, Xiaojuan; Nyström, Christina; Rundlöf, Anna-Klara; Fernandes, Aristi Potamitou; Björnstedt, Mikael; Dobra, Katalin

Free Radic Biol Med. 2006 Sep 15;41(6):874-85.
Elsevier
http://doi.org/10.1016/j.freeradbiomed.2006.04.031
http://hdl.handle.net/10616/47514

# Selenite induces apoptosis in sarcomatoid malignant mesothelioma cells through oxidative stress

Gustav Nilsonne, Xiaojuan Sun, Christina Nyström, Anna-Klara Rundlöf, Aristi Potamitou Fernandes, Mikael Björnstedt and Katalin Dobra[1]

Department of Laboratory Medicine, Karolinska University Hospital, F-46, Karolinska Institutet, S-141 86 Huddinge, Stockholm, Sweden.

**Running title:** Selective induction of apoptosis in sarcomatoid mesotheliomas

**Acknowledgments:** The authors are grateful to Ms Mervi Nurminen and Ms Ingrid Norman for skilful technical assistance, as well as to professor Anders Hjerpe for his unfailing support in all aspects of this study. This study was supported by grants from the Swedish Cancer and Allergy Fund, the Swedish Society of Medicine, and the Swedish Heart and Lung Association

[1] **Corresponding author:** Katalin Dobra, MD, PhD, Tel: +46-8-5858 5485, Fax: +46-8-5858 1025, e-mail: katalin.dobra@labmed.ki.se

# Selenite induces apoptosis in sarcomatoid malignant mesothelioma cells through oxidative stress

## Abstract

Malignant mesothelioma cells differentiate into sarcomatoid or epithelioid phenotypes. The sarcomatoid cell type is more resistant to chemotherapy and yields a worse prognosis. We have investigated whether selenite alone and in combination with doxorubicin induced apoptosis in variously differentiated mesothelioma cells. Selenite in concentrations that could potentially be administered to patients strongly inhibited the growth of the sarcomatoid mesothelioma cells (IC 50 = 7.5 μM), whereas epithelioid cells were more sensitive to doxorubicin. Benign mesothelial cells remained largely unaffected. Selenite potentiates doxorubicin treatment.. Apoptosis was the dominating mode of cell death. The toxicity of selenite was mediated by oxidative stress. Furthermore the activity of the thioredoxin system was directly dependent on the concentration of selenite. This offers a possible mechanism of action of selenite treatment. Our findings suggest that selenite is a promising new drug for the treatment of malignant mesothelioma.

**Keywords**: mesothelioma, phenotype, drug-resistance, apoptosis, selenium, thioredoxin reductase.

# Introduction

Malignant mesothelioma is a tumor arising from mesothelial cells following asbestos exposure. The tumor is aggressive and highly resistant to chemotherapy. Mesothelioma cells may differentiate into an epithelioid or a sarcomatoid phenotype. Presence of sarcomatoid cells in the tumor correlates to a poor prognosis. Furthermore, a survival advantage for patients receiving surgery and adjuvant chemotherapy has been confirmed only in patients with epithelioid morphology, and such therapy had no impact on survival in patients with sarcomatoid mesothelioma [1]. The ability of mesothelioma cells to differentiate into these two phenotypes has been retained in the cell lines STAV-AB (epithelioid) and STAV-FCS (sarcomatoid). Both sub-lines are derived from the same tumor, and their growth patterns depend on the serum composition [2].

A detailed and systematic molecular screening approach, based on suppression subtractive hybridization (SSH) and DNA array analyses, has uncovered important differences in the molecular basis of mesothelioma differentiation [3, 4]. Some of these differences may be further explored for therapeutical purposes. In particular, the thioredoxin system is highly upregulated in both STAV cell lines, with the epithelioid STAV-AB cells having the highest amounts of thioredoxin reductase-1 (TrxR1) reported so far [3]. Overexpression of thioredoxin 1 (Trx1) in malignant mesothelioma has also been reported using cDNA and mRNA microarray [5-7], and malignant mesothelioma tissue biopsies show immunoreactivity to both these proteins[8].

The thioredoxin system comprises Trx1, TrxR1, and NADPH. This system has the capacity to reduce protein disulfides in general. It plays an important role in the regulation of the redox balance in the cell, associating e.g. apoptosis to redox

mechanisms. TrxR1 is a key enzyme in selenium metabolism [9, 10] that generates indispensable selenium substrates for the synthesis of all selenoproteins. Glutathione peroxidase (GPx) is also a selenoenzyme with an important antioxidant role in the cell.

It has been hypothesized that one carcinogenic effect of asbestos is due to generation of reactive oxygen species. The exceptionally high expression of TrxR1 in mesothelioma cell lines indicates that the enhanced ability to maintain cellular redox status may give a survival advantage for transformed mesothelial cells. The modulation of cellular redox status thus emerges as a target for drug action.

This study aimed to investigate the consequences of altered redox balance on the viability of mesothelioma cells. We studied the effects of selenite, alone or in comparison with doxorubicin, measuring the viability of variously differentiated mesothelioma cells. We also measured apoptosis, ROS, and the effects on TrxR1 and GPx.

# Materials and methods

### *Chemicals*

Selenite ($Na_2SeO_3$), Tris-HCl, EDTA, HEPES, DMSO, sodium azide ($NaN_3$), $H_2O_2$, 5,5´dithiobis (nitrobenzoic acid) (DTNB), guanidine-HCl, bovine serum albumin, sodium deoxycholate (NaDOC), Biuret reagent, Glutathione (GSH), insulin from bovine pancreas, ascorbic acid, 2, 7-dichlorodihydrofluorescein diacetate (DCF) and NADPH were all purchased from Sigma (St. Louis, USA). Doxorubicin (Adriamycin®) was obtained from Pharmacia & Upjohn (Stockholm, Sweden). Baker´s yeast glutathione reductase (GR) and DCFH-DA (5(6)-Carboxy-2',7' -dichlorofluorescein diacetate) was obtained from Fluka (Buchs, Switzerland). *E. coli* Trx1 was purchased from Promega (Leiden, the Netherlands). The specific antibody to Trx1 was obtained from IMCO Corporation (Stockholm, Sweden), and the anti-TrxR1 antibody was purchased from Upstate Biotechnology (NY, USA). WST-1 colorimetric reagent was obtained from Roche (Penzberg, Germany). Gentamicin and RPMI 1640 medium was obtained from Invitrogen Corporation (Carlsbad, CA, USA). The Annexin V kit was obtained from Caltag Laboratories, (Burlingame, CA, USA).

*Cell culturing and characterization of growth pattern:*

Experiments were performed on a well-established *in vitro* model of mesothelioma differentiation consisting of the two malignant mesothelioma cell sub-lines STAV-AB and STAV-FCS [11]. STAV-AB is grown in human AB serum and has epithelioid morphology, whereas STAV-FCS is grown in Fetal Calf Serum (FCS) and has sarcomatoid morphology (Fig. 1). Furthermore, we have included three other mesothelioma cell lines, two adenocarcinoma cell lines and two short-term cultures of

benign mesothelial cells. The M9K and M28K mesothelioma cell lines were kindly provided by Dr. K. Linnainmaa (Helsinki, Finland). The ZL34 mesothelioma cell line and the WART adenocarcinoma cell line were provided by Dr. J. Klominek (Huddinge, Sweden). The MCF7 breast cancer cell line was purchased from the American Type Culture Collection (ATCC, Rockville, MD, USA). The cultures of benign mesothelial cells were derived from cytological material sent to the laboratory for examination. The local ethical committee approved this study in accordance with the ethical standards of the Helsinki Declaration of 1975, as revised in 1983.

Tumor cells were cultivated in 75 $cm^2$ flasks (Sarstedt, Newton, USA) in RPMI 1640 medium supplemented with Gentamicin and 10% serum under conditions of 37ºC and 5% $CO_2$. Cell morphology was assessed by phase-contrast microscopic examination and immunostaining with two differentiation markers; vimentin and cytokeratin, as described by Dobra et al. [11], verifying the preserved differences in phenotype. For analysis of levels of reactive oxygen species, cells were grown directly on glass slides, and the experiment was performed at 80% confluence.

*Assay of cytotoxicity:*

The WST-1 colorimetric reagent was used to measure cell viability. This reagent is cleaved by mitochondrial enzymes in living cells. The cleavage products are fluorescent at 450 nm. Samples were analysed in a microplate reader, the fluorescence at 650 nm was measured and subtracted from that at 450 nm to compensate for differences in background absorbance.

The effect of doxorubicin, selenite and their combination on the *in vitro* growth of mesothelioma cells with various differentiations was determined using the STAV-AB and STAV-FCS cell lines. The cells were distributed on 96-well microplates with an equal number of approx. 40,000 cells in each well. They were then incubated for up to 76 h with selenite and/or doxorubicin. Measurements of cytotoxicity were made at 24-hour intervals, starting at 4 h. Initially experiments were conducted with selenite concentrations of 1, 2.5, 5, 10, and 30 µM. IC 50 was calculated from the obtained dose response curve. Similarly, doxorubicin was tested in concentrations of 0.2, 0.6, and 1.2 µg/ml, corresponding to 0.33, 1 and 2 µM, respectively [12].

Based on results of these trials, an experiment was set up where the cells were incubated with combinations of 5 and 10 µM of selenite and 0.2 and 0.6 µg/ml of doxorubicin, as well as an untreated control. All experiments were carried out three times in quadruplicate.

To investigate whether the cytotoxic effect of selenite could be abrogated by an antioxidant, cells were treated with 7,5 µM of selenite using the same procedure as described above, and ascorbic acid was added in concentrations ranging between 0 µM and 1 mM.

*Assessment of apoptosis:*

STAV-FCS and STAV-AB cells were distributed in equal amounts of approx. 450,000 in 25 $cm^2$ flasks (Sarstedt, Newton, USA) and incubated with 1, 5, 10 and 30 µM of selenite. Cells were harvested after 24 and 48 hours and subjected to morphological examination and FACS analysis. Similarly, cells of both sub lines were treated with 5 and 10 µM of selenite combined with 0.2 and 0.6 µg/ml of doxorubicin. After 24 and 48 h, the cells

were harvested and analyzed independently using morphological methods and FACS-analysis, and compared to an untreated control population. Both experiments were repeated three times.

*i.) Morphological examination* - For every concentration, two cytospin preparations were made. Slides were allowed to dry and thereafter fixed for 30 seconds in 100% acetone followed by 10 min in 99.5% ethanol. After fixation, cells were stained with Giemsa dye. All slides were randomized and examined morphologically in a double-blind manner. Pyknosis (karyopyknosis) was defined as shrunken nuclei and condensation of the nuclear chromatin, indicating that the cells undergo programmed cell death. The pyknotic index was determined as the percentage of cells with pyknotic nuclei. Cells with more than one nucleus or without cytoplasm were not counted.

*ii.) Fluorescence-activated cell sorting (FACS)* - FACS examination was conducted using the Annexin V/Propidium Iodide (PI) analysis. Annexin V labels cells that demonstrate externalisation of phosphatidylserine on the plasma membrane, as an early sign of apoptosis. The parallel staining with propidium iodide (PI) labels those cells that have increased permeability of the cell membrane, as a sign of cell decay. This represents a later phase of apoptosis. When the dying cells begin to disintegrate, it is not possible to distinguish between apoptotic and necrotic cells using this analysis.

The procedure was carried out according to the manufacturer's instructions. Briefly, $10^5$ cells were pelleted, washed twice with PBS and resuspended in 100 µl Annex-B binding buffer. 5 µl of Annexin V and 5 µl of PI were added followed by incubation in the dark for 25 min. 400 µl Annex-B were added and the samples were immediately analyzed on

a FACS cytometer (Becton Dickinson, Mountain View, CA, USA), using the Cell Quest software.

***Enzyme activity analysis:***

*Preparation of cell homogenates* – Cell pellets were resuspended in a buffer (50 mM Tris-HCl, pH 7.6 and 1 mM EDTA) while kept on ice, followed by sonication and centrifugation at 25'000 × g for 10 min at 2°C. The supernatants were transferred to new tubes for enzyme activity measurements. The protein concentrations in the cell homogenates were determined by the Biuret method [13].

*TrxR1 enzyme activity assay* - The TrxR1 enzyme activity in the cell homogenates was measured through a coupled reaction according to Holmgren and Björnstedt [14]. From each homogenate 100 µg protein was incubated with 80 mM HEPES (pH 7.5), 0.9 mg/ml NADPH, 6 mM EDTA, 2 mg/ml insulin, and 10 µM E.coli Trx1 at 37°C for 20 minutes in a final volume of 120 µl. The reaction was terminated by the addition of 500 µl DTNB (0.4 mg/ml) with 6 M guanidine-HCl in 0.2 M Tris-HCl pH 8.0. The absorbance at 412 nm was measured within 20 min. The TrxR1 in the cell homogenates, using NADPH as a cofactor, reduced the oxidized Trx1 added. The reduced Trx1 then spontaneously reduced disulfides in insulin. The dithiols formed in insulin was visualized by the addition of DTNB. DTNB was reduced to $D^-$ and $TNB^+$ by the dithiols formed in insulin.

*GPx enzyme activity assay* - The GPx enzyme activity was measured through a coupled reaction described by Lawrence and Burk [15]. A modified protocol was created to fit a 96 well plate. 100 µg protein from each cell homogenate was incubated for 3 min at 25°C with 0.1 M Tris-HCl buffer (pH 7.6), 2 mM EDTA, 2 mM NaN3, 4 mM GSH, 10

units of GR and 0.8 mM NADPH in a total volume of 195 µl. After the incubation 5 µl of the reagent $H_2O_2$ was added to a concentration of 10 mM as a substrate for the GPx enzyme. The GPx reduced $H_2O_2$ to $H_2O$ by oxidizing two GSH into GSSG. GR then reduce GSSG into two GSH again oxidizing NADPH, the oxidation of NADPH into $NADP^+$ was measured kinetically at 340nm as an indirect measure of the GPx activity.

*Measurement of cellular redox status* – For *in vivo* detection of intracellular reactive oxygen species (ROS) induction, the fluorescent probe 2, 7-dichlorodihydrofluorescein diacetate (DCF) was used. Cells were exposed to 5, 7.5 and 21 µM selenite for various times (4, 8, and 12h), followed by 15 min incubation in the presence of 10 µM DCFH-DA probe, dissolved in a small volume of DMSO. The induction of ROS was monitored qualitatively by confocal laser microscopy. The excitation and emission wavelengths were 488 and 568 nm, respectively. Cells stimulated with 0.1 µM $H_2O_2$ were used as positive controls.

*Immunocyto- and histochemical analysis of the expression of Trx1 and TrxR1* – Cytological preparations were performed on 15 pleural effusions, comprising 5 malignant mesotheliomas, 5 adenocarcinomas and 5 benign mesothelial proliferations. Immunocytochemical reactions were performed on air-dried, acetone- and 95% ethanol-fixed cytospin preparations. Immunohistochemical analysis was performed on 9 native biphasic malignant mesothelioma tissue specimens from our mesothelioma bank, sampled by Dejmek et al. [16]. The histological sections were routinely processed, formalin fixed and paraffin-embedded.

Antigen retrieval was performed in 10mM sodium citrate buffer, pH 6.0 at 95°C. Endogenous peroxidase activity was abolished by 0.6-0.75 % $H_2O_2$ in methanol for 30 minutes and non-specific binding of antibodies was blocked by 3% normal rabbit or mouse serum. The cells were then incubated with specific antibodies to Trx1 (1:50), and to TrxR1 (1:100), respectively. Antigen-antibody reaction products were visualized with the streptavidin-biotin-peroxidase method with diaminobenzidine as substrate-chromogen (ChemMate Detection Kit, DAKO).

Negative controls were obtained by using the specific antibodies after pre-incubation with excess amounts of Trx1 and TrxR1 proteins, respectively. All moderate or strong staining was evaluated as positive. Weak staining or focal reactivity in dispersed cells was considered as negative.

***Statistics***

Data were evaluated by one-way ANOVA tests and Tukey-Kramer Honestly Significant Difference tests. The null hypothesis of no difference was rejected at a significance level of $p<0.05$. Confidence intervals for the pycnotic indices were calculated using the statistic $(x-p)/\sqrt{(p(1-p)/n)}$.

# Results

### *Characterization of cells*

The doubling time was comparable between the STAV AB and STAV FCS cell sub lines.- When the cells were harvested, they were carefully examined to ensure that the growth patterns remained epithelioid and sarcomatoid, respectively. STAV-AB cultures have a cobblestone appearance whereas STAV-FCS cells have a length:width ratio exceeding 2:1. Immunocytochemical analysis showed that the epithelioid STAV-AB cells were strongly reactive to cytokeratin antibodies, but the vimentin staining dominated in the fibroblast-like STAV-FCS cells.

### *Doxorubicin selectively inhibits the growth of epithelioid but not sarcomatoid mesothelioma cells*

To investigate the effect of doxorubicin on mesothelioma cells of epithelioid and sarcomatoid differentiation, the STAV-AB and STAV-FCS cell lines were treated with increasing doxorubicin concentrations (0.2-1.2 μg/ml), and the number of viable cells was assayed after 28 and 52 hours. The epithelioid cells showed a dose- and time-dependent growth inhibition. Already after 28 hours a significant reduction of cell viability was detected using 1.2 μg/ml doxorubicin. These cells were increasingly growth inhibited after 52 hours (Fig. 2A). In contrast, the sarcomatoid cells did not respond to the treatment. The proliferation rate of these resistant cells rather seemed to increase when treated with the highest concentration of doxorubicin (1.2 μg/ml), although the difference was not statistically significant (Fig. 2B).

***Selenite inhibits the growth of both mesothelioma phenotypes in a dose- and time-dependent manner***

The effect of selenite on cell growth was assayed after 28 and 52 h, using concentrations ranging from 1-30 μM. Both the epithelioid and the sarcomatoid cell sub lines were inhibited when treated with 5-30 μM of selenite. The sarcomatoid cells were significantly more sensitive to lower selenite concentrations already after 28 h (Fig. 2C). IC 50 as determined after 28 h was 7.5 μM for the sarcomatoid cell line and 21 μM for the epithelioid cells. At 52 h, the pattern was similar and the inhibition was stronger (data not shown). At low doses (1-5 μM), transient growth stimulation was observed in both phenotypes.

***Several tumor cell lines respond well to selenite treatment, whereas benign mesothelial cells are less sensitive***

To investigate whether the effects of selenite treatment could be generalized to other cancer cells, a cytotoxicity test was conducted on several other cell lines. We used three mesothelioma cell lines, two adenocarcinoma cell lines and two short-term cultures of benign mesothelial cells. They were treated for 24 and 48 h with 7.5 μM of selenite. Both adenocarcinomas were inhibited to less than 40% of control in 24 h, and one mesothelioma dropped to 5% of control. After 48 h, none of the malignant cell lines exceeded 5% of the viability of the controls. The benign mesothelial cells were growth stimulated at 24 h, and 69% or more, relative to control, remained viable after 48 h (Fig. 2D).

***Selenite potentiates the toxic effect of doxorubicin***

Treatment with selenite and doxorubicin was combined to assess whether they have synergistic effects. This treatment inhibited epithelioid cells strongly. Although the effect was limited at 28 h, treatment with 0.2 or 0.6 µg/ml of doxorubicin combined with 10 µM of selenite for 52 h caused a dramatic loss of viability. Treatment with the same concentrations of doxorubicin and 5 µM of selenite yielded viability ranging between 20% and 40% of control (Fig. 2E). In contrast, sarcomatoid cells were inhibited already at 28 h. Of the cells treated with doxorubicin together with 5 or 10 µM of selenite, respectively, around 90% and 60% of the cells were still viable relative to control at 28 h, dropping to around 60% and 50% at 52 h (Fig. 2F).

***Selenite induces apoptosis in mesothelioma cells***

STAV-AB and STAV-FCS cells were treated with increasing selenite concentrations and the amount of apoptotic cells was assessed by morphological investigation and by FACS analysis of Annexin-V positive cells. Morphological analysis shows significantly increased apoptosis, as judged from the proportion of pyknotic cells, at 10 and 30 µM of selenite for the epithelioid cells (Fig. 3A) and at 5, 10 and 30 µM of selenite for the sarcomatoid cells (Fig. 3B). At 10 µM, the percentage of cells with apoptotic characteristics is close to 40% for both phenotypes. At 30 µM it increases to between 60% and 80%. Necrosis as judged morphologically by cell swelling and loss of chromatin patterns occurred in a small number of cells only and was completely subordinate to death by apoptosis.

FACS analysis shows that both the epithelial (Fig. 3 C) and the sarcomatoid (Fig. 3 D) phenotypes undergo apoptosis in a time and dose dependent manner. The kinetics of the

apoptotic changes however differed substantially between the phenotypes. At 28 hours, the proportion of early apoptotic cells, corresponding to the lower right quadrant, was much higher in the sarcomatoid phenotype (Fig. 3 D) than in the epithelioid phenotype (Fig. 3 C). The sarcomatoid cells showed more advanced changes with a substantial proportion of cells in the upper right quadrant, corresponding to late apoptosis (Fig. 3D). At 52 hours, similar pattern of distribution of early and late apoptotic cell populations have developed also in the epithelioid cells. The morphological investigation of these late apoptotic or pyknotic cells, show a good correlation with the FACS analysis (Fig. 3).

***The combination of selenite and doxorubicin induces apoptosis in mesothelioma cells of both phenotypes***

Both cell sub lines demonstrate significantly increased apoptosis, as measured morphologically, after treatment with 10 µM selenite and 0.6 or 1.2 µg/ml of doxorubicin at 48 h. These samples had proportions of 6%-10% of apoptotic cells when judged morphologically. FACS analysis of PI uptake was not possible due to doxorubicin fluorescence. When estimated from the binding of Annexin V, to the number of apoptotic cells was 44% among the epithelioid cells and 24% among the sarcomatoid cells.

***Selenite decreases TrxR1 and GPx activity***

The activity and amount of TrxR1 and GPx were assayed using two different methods. Both cell lines have an exceptionally high expression of TrxR1. It is highest in the epithelioid cell line where it exceeds 12 µg/mg of total protein. When treated with 10 µM selenite the activity decreased dramatically, reaching about 50% in the epithelioid

cells, and about 80% in the sarcomatoid cells. At 30 μM only a small fraction of the original activity was still detectable (Fig. 4A).

The activity of GPx was similar in the two phenotypes, and it increased when the cells proliferated in low concentrations of selenite. The activity was, however, inhibited already at 2.5 μM, the sarcomatoid cells being somewhat more sensitive than the epithelioid ones. At 10 and 30 μM the activity was less than 30% of the original levels (Fig. 4B).

***Selenite toxicity is mediated by oxidative stress***

We determined the reactive oxygen species (ROS) generation in the presence or absence of selenite (Fig. 5a). Sarcomatoid mesothelioma cells exposed to selenite have shown a time and dose dependent increase in DCF fluorescence intensity compared to the untreated paternal cells. A differential effect of selenite was observed on the two cell phenotypes through the experiment, with selective ROS induction in the most resistant sarcomatous phenotype. In contrast, a reduction of DCF fluorescence intensity was observed in the epithelioid STAV-AB cell sub-line following selenite exposure. The toxicity of selenite could be completely reversed by the addition of ascorbic acid, which is an antioxidant (fig 6).

***Detection of Trx1 and TrxR1 in tumor specimens***

The immunocytochemical investigation revealed strong to moderate immunoreactivity for both Trx1 and TrxR1 antibodies in malignant mesotheliomas and adenocarcinomas, whereas benign mesothelial cells were negative (Fig.7). However, reactive mesothelial cell samples displayed scattered cells with weak positive staining.

This corresponds well to a study by Kahlos et al. [8], where TrxR1 immunostaining could also not be demonstrated in benign mesothelium.

Immunohistochemical analysis on biphasic malignant mesothelioma tissue specimens showed profound differences in the TrxR1 protein levels of epithelioid and sarcomatous tumor components. Marked reactivity was noted in the epithelial component of all biphasic tumors (Fig. 8), but the spindle-shaped sarcomatous tumor components remained largely unstained.

## Discussion

Malignant mesothelioma is a tumor that may exhibit two phenotypes – epithelioid and sarcomatoid – which seem to have different mechanisms for cancer progression [4] and respond differently to therapy. Presence of the sarcomatoid phenotype in a tumor is correlated to therapy resistance and a worse prognosis. Mesothelioma responds poorly and often only partially to treatment [17, 18], which may be explained by the tumor cell heterogeneity. Our previous molecular characterization reveals profound differences between the phenotypes [4]. This characterization makes it possible to find drug targets that are specific for the respective tumor component. One such possible target is the thioredoxin system, which is both abundantly and differentially expressed in the two mesothelioma phenotypes.

Treatment of malignant mesothelioma is most often based on a combination of several drugs. Doxorubicin is an anthracycline that is often included in such chemotherapy regimens. It has several mechanisms, one of which is the formation of free radicals, leading to oxidative stress [19]. High-dose doxorubicin causes excessive toxicity, particularly to the heart [20]. In this study, the sarcomatoid cells were resistant to doxorubicin, while the epithelioid cells were sensitive, which correlates well to both clinical experience [17, 18] and *in vitro* studies. IC 50 values of doxorubicin for mesothelioma cell lines ranging between 0.01 and 1.85 μM have been reported [21-24], and in comparison both our cell sub lines appear to be extraordinarily resistant. In fact, the sarcomatoid cells continued to proliferate when treated with the highest dose given (2 μM). A similar result has been reported by Hedges et al [21]. For therapeutical purposes, serum doxorubicin concentrations ranging from approx. 0.025 to 2 μM are considered

useful [19], and cytotoxic effects on the sarcomatoid components would then not be expected.

In contrast with the above findings the otherwise therapy-resistant sarcomatoid cells were sensitive to selenite with a striking loss of viability (IC 50 = 7.5 μM), when selenite ($SeO_3^{2-}$) was administered as a sodium salt. The epithelioid cells were not as sensitive (IC 50 = 21 μM). The effect of selenite was dose-dependent. We confirmed these results using three additional mesothelioma cell lines and two adenocarcinoma cell lines, all of which were highly sensitive when treated with 7.5 μM of selenite. In contrast, short-term cultures of benign mesothelium tolerated this concentration well. At lower concentrations we observed a transient growth stimulation, which may be a consequence of suboptimal amounts of selenium in standard cell culture conditions [25].

We have shown that selenite induces the formation of ROS in the sarcomatoid cells, while in the epithelioid cells, with their higher levels of the thioredoxin system, this could not be seen by DCF labeling. It was possible to eliminate the toxic effect by the addition of an antioxidant (ascorbic acid) indicating that the cytotoxic effect of selenite is mediated by oxidative stress. This result is consistent with previous reports [26, 27]. Using independent methods we have also confirmed that the mode of cell death is apoptosis.

Selenite is a small ion that diffuses easily over plasma membranes to reach the intracellular compartment. In the presence of TrxR1 or thiol groups it is readily reduced into selenide ($HSe^-$), which in the presence of oxygen undergoes redox cycling, causing rapid and massive non-stoichiometric oxidation of NADPH [28]. Furthermore, selenite may directly redox cycle with thiols to cause superoxide generation [29] and loss of

protein structure. Unbalanced generation of ROS such as superoxide will damage cellular constituents and induce apoptosis as a consequence [30]. The oxidation of thiols into disulfides may cause conformational changes in the affected proteins, which can render them unable to exert their normal function. This adds to the previously shown effects of selenium on mesothelioma cells related to the expression of Selenoprotein 15 (SEP15) [31], where cells expressing less SEP15 were less responsive to the effects of selenium.

Both malignant mesothelioma cell sub-lines used in this study express exceptionally high levels of TrxR1. The epithelioid cell line expresses twice as much as the sarcomatoid cell line. The mechanism of selenite toxicity is likely mediated in part by oxidation of thiols, with a resulting generation of ROS. Selenite will oxidize thiol groups, and these will be regenerated by TrxR1. In doing so, the Trx1 will become oxidized. When oxidized, Trx1 causes release and activation of Apoptosis Signal Regulating Kinase 1 (ASK-1) [32].

On the other hand, a high level of TrxR1 or a capacity to induce the activity has recently been shown to correlate with cell survival after exposure to increasingly toxic levels of selenium [33-35], In the present study we show a similar correlation since the epithelioid cells were more resistant to selenite. The protective effect of TrxR1 is likely explained by three different mechanisms, namely detoxification of selenite by reduction to elementary selenium, restoring intracellular thiols lost in redox cycling, and the detoxification of ROS, also formed during redox cycling.

Intracellular thiols thus have a double-edged effect. In the context of selenite treatment, they may either protect or damage the cell, possibly depending on their amount

and forms. This hypothetical model for the actions of selenite and the thioredoxin system is summarized in Fig. 9.

When the cells were exposed to selenite, cell survival was seen in the cells with the highest levels of TrxR1 and GPx activity. The damaging effects of selenite were amplified by the dose-dependent decrease in activity of both these enzymes. The remaining level of TrxR1 and GPx activity correlated well to the decrease of cell viability.TrxR1 has several well-described prosurvival effects. The high levels seen in mesothelioma may reflect a functional adaptation to an adverse redox environment, leading to increased dependence on the function of this enzyme. These cells may therefore be more sensitive to a decreased activit of TrxR1. Similarly; the decrease in GPx activity caused by selenite may play a part in the cytotoxic effect.

Selenite treatment potentiated the toxic effect of doxorubicin and yielded a dramatic loss of viability in both cell types. Due to the heteroscedastic distribution of data, we did not analyze whether there was a statistically significant synergism. This effect is likely explained in part by the decreased activity of TrxR1 induced by selenite, since a high activity of TrxR1 is protective against the cytotoxic effects of doxorubicin [36, 37].

Overexpression of Trx1 has been reported in several mesothelioma cell lines using cDNA and mRNA microarray [5-7], and distinct immunohistochemical reactivities for Trx1 and TrxR1 are common in malignant mesothelioma cell lines and tumor biopsies [8]. It can then be expected that the described sensitivity to selenite is common in

malignant mesotheliomas, while the benign mesothelium remains unaffected by such treatment.

Selenium toxicity has been relatively well studied. The main symptoms of chronic toxicity are brittleness of hair and nails and garlic breath. Yang et al. have shown that symptoms of selenium toxicity may be experienced at blood concentrations ranging from 1.05 mg/l, corresponding to 13.3 μM, as measured by changes in the fingernails [38]. Recently published data [39] indicate that doses up to 3200 μg/day over long periods of time can be tolerated, although mild symptoms including dizziness, brittle nails and hair, and garlic breath were reported by a few of the participants is the study. Blood selenium concentrations exceeding the 7.5 μM that we have used can probably be maintained safely in patients in the course of cancer therapy. The specific toxicity of selenite has not been systematically studied in humans, and therefore titration of maximal tolerable dose (MTD) would be necessary before commencing treatment. Concentrations ranging up to around 2 μM may stimulate proliferation of tumor cells. Transient growth stimulation may thus be expected when commencing such therapy. It may therefore be advisable to combine selenite treatment with one or more antimitotic cytostatics.

We show that when selenite is administered in clinically tolerable concentrations to mesothelioma cell lines, it generates ROS, oxidizes thiols and decreases the activity of the thioredoxin system. Consequently, apoptosis signaling pathways are activated, most likely through the mitochondrial pathway and ASK-1 signaling. The result is a striking loss of viability, especially in cells of the doxorubicin-resistant sarcomatoid phenotype. The selenium also seems to potentiate simultaneously

administered doxorubicin with effects also in the epithelioid cells. This is a promising path towards new therapeutic possibilities.

Studies aiming at a detailed characterization of the selenite-induced apoptosis mechanisms are in progress at our laboratory. Furthermore, the hypothesis should be investigated using *in vivo* systems that allow analysis of a wide range of possible effects of selenium, for example on tumor vascularization. Clinical trials with the prospect of taking advantage of these effects are imminent.

## Abbreviations

| | |
|---|---|
| AB | Human AB serum |
| Adeno | Adenocarcinoma |
| ASK-1 | Apoptosis Signal Regulating Kinase 1 |
| DCF | 2', 7'-dichlorodihydrofluorescein diacetate |
| DCFH-DA | 5(6)-carboxy-2', 7'-dichlorodihydrofluorescein diacetate |
| DMSO | Dimethyl sulfoxide |
| DTNB | 5, 5'dithiobis(nitrobensoic acid) |
| EDTA | Ethylenediaminetetraacetic acid |
| FACS | Fluorescence Activated Cell Sorting |
| FCS | Fetal Calf Serum |
| GPx | Glutathione Peroxidase |
| GR | Glutathione Reductase |
| GSH | Glutathione (reduced) |
| GSSG | Glutathione (oxidized) |
| HEPES | 4-(2-hydroxyethyl)-1-piperazineethanesulfonic acid |
| MM | Malignant mesothelioma |
| NaDOC | Sodium Deoxycholate |
| PI | Propidium Iodide |
| ROS | Reactive Oxygen Species |
| SD | Standard Deviation |
| SEM | Standard Error of the Mean |
| SEP15 | Selenoprotein 15 |

| | |
|---|---|
| Trx1 | Thioredoxin 1 |
| TrxR1 | Thioredoxin Reductase 1 |
| WST-1 | Cell Proliferation Reagent |

# References

[1] Ceresoli, G. L.; Locati, L. D.; Ferreri, A. J. M.; Cozzarini, C.; Passoni, P.; Melloni, G.; Zannini, P.; Bolognesi, A.; Villa, E. Therapeutic outcome according to histologic subtype in 121 patients with malignant pleural mesothelioma. *Lung cancer*. **34:**279-287; 2001.

[2] Klominek, J.; Robért, K. H.; Hjerpe, A.; Wickström, B.; Gahrton, G. Serum-dependent Growth Patterns of Two, Newly Established Human Mesothelioma Cell Lines. *Cancer res*. **49:**6118-6122; 1989.

[3] Sun, X.; Dobra, K.; Björnstedt, M.; Hjerpe, A. Upregulation of 9 genes, including that for thioredoxin, during epithelial differentiation of mesothelioma cells. *Differentiation*. **66:**181-188; 2000.

[4] Sun, X.; Wei, L.; Liden, J.; Hui, G.; Dahlman-Wright, K.; Hjerpe, A.; Dobra, K. Molecular characterization of tumour heterogeneity and malignant mesothelioma cell differentiation by gene profiling. *J Pathol*. **207:**91-101; 2005.

[5] Rihn, B. H.; Mohr, S.; McDowell, S. A.; Binet, S.; Loubinoux, J.; Galateau, F.; Keith, G.; Leikauf, G. D. Differential gene expression in mesothelioma. *FEBS letters*. **480:**95-100; 2000.

[6] Mohr, S.; Bottin, M. C.; Lannes, B.; Neuville, A.; Bellocq, J. P.; Keith, G.; Rihn, B. H. Microdissection, mRNA amplification and microarray: a study of pleural mesothelial and malignant mesothelioma cells. *Biochimie*. **86:**13-19; 2004.

[7] Mohr, S.; Keith, G.; Galateau-Salle, F.; Icard, P.; Rihn, B. H. Cell protection, resistance and invasiveness of two malignant mesotheliomas as assessed by 10K-microarray. *Biochim Biophys Acta*. **1688:**43-60; 2004.

[8] Kahlos, K.; Soini, Y.; Saily, M.; Koistinen, P.; Kakko, S.; Paakko, P.; Holmgren, A.; Kinnula, V. L. Up-regulation of thioredoxin and thioredoxin reductase in human malignant pleural mesothelioma. *Int J Cancer*. **95:**198-204; 2001.

[9] Holmgren, A.; Arnér, E.; Åslund, F.; Björnstedt, M.; Zhong, L.; Ljung, J.; al., e. (1996). Redox regulation by the thioredoxin and glutaredoxin systems. In Oxidative stress in cancer, AIDS, and neurodegenerative diseases, L. Montagnier, R. Olivier, C. Pasquier and e. al., eds. (Paris: Marcel Decker), pp. 229-246.

[10] Björnstedt, M.; Kumar, S.; Bjorkhem, L.; Spyrou, G.; Holmgren, A. Selenium and the thioredoxin and glutaredoxin systems. *Biomed Environ Sci*. **10:**271-279; 1997.

[11] Dobra, K.; Nurminen, M.; Hjerpe, A. Growth factors regulate the expression profile of their syndecan co-receptors and the differentiation of mesothelioma cells. *Anticancer Res*. **23:**2435-2444; 2003.

[12] Liu, W.; Bodle, E.; Chen, J. Y.; Gao, M.; Rosen, G. D.; Broaddus, V. C. Tumor Necrosis Factor-Related Apoptosis-Inducing Ligand and Chemotherapy cooperate to Induce Apoptosis in Mesothelioma Cell Lines. *Am. J. Respir, Cell and Mol. Biol*. **25:**111-118; 2001.

[13] Gornall, A. G.; Bardawill, C. J.; David, M. M. Determination of serum proteins by means of the biuret reaction. *J. Biol. Chem*. **177:**751-766; 1949.

[14] Holmgren, A.; Björnstedt, M. Biothioles. *Methods in Enzymology*. **252:**199-208; 1995.

[15] Lawrence, R. A.; Burk, R. F. Glutathione peroxidase activity in selenium-deficient rat liver. *Biochem Biophys Res Commun*. **71:**952-958; 1976.

[16] Dejmek, A.; Brockstedt, U.; Hjerpe, A. Optimization of a battery using nine immunocytochemical variables for distinguishing between epithelial mesothelioma and adenocarcinoma. *Apmis*. **105:**889-894; 1997.

[17] Berghmans, T.; Paesmans, M.; Lalami, Y.; Iouviaux, I.; Luce, S.; Mascaux, C.; Meert, A. P.; Sculier, J. P. Activity of chemotherapy and immunotherapy on Malignant Mesothelioma: a systematic review of the literature with meta-analysis. *Lung Cancer*. **38:**111-121; 2002.

[18] Tomek, S.; Manegold, C. Chemotherapy for malignant pleural mesothelioma: past results and recent developments. *Lung Cancer*. **45 suppl 1:**S103-119; 2004.

[19] Gewirtz, D. A. A critical evaluation of the mechanisms of action proposed for the antitumor effects of the anthracycline antibiotics adriamycin and daunorubicin. *Biochemical Pharmacology*. **57:**727-741; 1999.

[20] Kosty, M. P.; Herndon, J. E.; Vogelzang, N. J.; Kindler, H. L.; Green, M. R. High-dose doxorubicin, dexrazoxane, and GM-CSF in malignant mesothelioma: a phase II study - Cancer and Leukemia Group B 9631. *Lung cancer*. **34:**289-295; 2001.

[21] Hedges, K. L.; Morré, D. M.; Wu, L.; Morré, J. Adriamycin tolerance in human mesothelioma cell lines and cell surface NADH oxidase. *Life Sciences*. **73:**1189-1198; 2003.

[22] Isobe, H.; Wellham, L.; Sauerteig, A.; Stridhar, K. S.; Ramachandran, C.; Krishan, A. Doxorubicin retention and chemoresistance in human mesothelioma cell lines. *Int J Cancer*. **57:**581-585; 1994.

[23] Brophy, P. F.; Keller, S. M. Adriamycin enhanced in vitro and in vivo photodynamic therapy of mesothelioma. *J Surg Res*. **52:**631-634; 1992.

[24] Griffin, T. W.; Socl, M.; Collins, J.; Fernandes, J.; Maher, V. E. Combined antitumour therapy with the chemotherapeutic drug doxorubicin and an anti-transferrin receptor immunotoxin: in vitro and in vivo studies. *J Immunother*. **11:**12-18; 1992.

[25] Leist, M.; Raab, B.; Maurer, S.; Rosick, U.; Brigelius-Flohe, R. Conventional cell culture media do not adequately supply cells with antioxidants and thus facilitate peroxide-induced genotoxicity. *Free Radic Biol Med*. **21:**297-306; 1996.

[26] Shen, H. M.; Yang, C. F.; Ong, C. N. Sodium selenite-induced oxidative stress and apoptosis in human hepatoma HepG2 cells. *Int J Cancer*. **81:**820-828; 1999.

[27] Shen, H.; Yang, C.; Liu, J.; Ong, C. Dual role of glutathione in selenite-induced oxidative stress and apoptosis in human hepatoma cells. *Free Radic Biol Med*. **28:**1115-1124; 2000.

[28] Kumar, S.; Björnstedt, M.; Holmgren, A. Selenite is a substrate for calf thymus thioredoxin reductase and thioredoxin and elicits a large non-stoichiometric oxidation of NADPH in the presence of oxygen. *Eur J Biochem.* **207:**435-439; 1992.

[29] Spallholz, J. E. Free radical generation by selenium compounds and their prooxidant toxicity. *Biomed Environ Sci.* **10:**260-270; 1997.

[30] Orrenius, S. Mitochondrial regulation of apoptotic cell death. *Toxicology Letters*. **149:**79-23; 2004.

[31] Apostolou, S.; Klein, J. O.; Mitsuuchi, Y.; Shetler, J. N.; Poulikakos, P. I.; Jhanwar, S. C.; Kruger, W. D.; Testa, J. R. Growth inhibition and induction of apoptosis in mesothelioma cells by selenium and dependence on selenoprotein SEP15 genotype. *Oncogene*. **23:**5032-5040; 2004.

[32] Saitoh, M.; Nishitoh, H.; Fujii, M.; Takeda, K.; Tobiume, K.; Sawada, Y.; Kawabata, M.; Miyazono, K.; Ichijo, H. Mammalian thioredoxin is a direct inhibitor of apoptosis signal-regulating kinase (ASK) 1. *Embo J.* **17:**2596-2606; 1998.

[33] Björkhem-Bergman, L.; Jonsson, K.; Eriksson, L. C.; Olsson, J. M.; Lehmann, S.; Paul, C.; Björnstedt, M. Drug-resistant human lung cancer cells are more sensitive to selenium cytotoxicity. Effects on thioredoxin reductase and glutathione reductase. *Biochem Pharmacol.* **63:**1875-1884; 2002.

[34] Jonsson-Videsater, K.; Bjorkhem-Bergman, L.; Hossain, A.; Soderberg, A.; Eriksson, L. C.; Paul, C.; Rosen, A.; Bjornstedt, M. Selenite-induced apoptosis in doxorubicin-resistant cells and effects on the thioredoxin system. *Biochem Pharmacol*. **67:**513-522; 2004.

[35] Madeja, Z.; Sroka, J.; Nyström, C.; Björkhem-Bergman, L.; Nordman, T.; Damdipolous, A.; Nalvarte, I.; Eriksson, L. C.; Spyrou, G.; Olsson, J. M.; Björnstedt, M. The role of thioredoxin reductase activity in selenium induced cytotoxicity. *Submitted*. 2004.

[36] Wang J, K. M., Sakurada K, Imamura M, Moriuchi T, and Hosokawa M Possible roles of an Adult T-cell Leukemia (ATL)-Derived Factor/Thioredoxin in the Drug Resistance of ATL to Adriamycin. *Blood*. **89:**2480-2487; 1997.

[37] Yokomizo A, O. M., Nanri H, Makino Y, Ohga T, Wada M, Okamoto T, Yodoi J, Kuwano M, Kohno K Cellular levels of thioredoxin associated with drug sensitivity to cisplatin, mitomycin C, doxorubicin, and etoposide. *Cancer Res*. **55:**4293-4296; 1995.

[38] Yang, G.; Yin, S.; Zhou, R.; Gu, L.; Yan, B.; Liu, Y. Studies of safe maximal daily dietary Se-intake in a seleniferous area in China. Part II: Relation between Se-intake and the manifestation of clinical signs and certain biochemical alterations in blood and urine. *J Trace Elem Electrolytes Health Dis*. **3:**123-130; 1989.

[39] Reid, M. E.; Stratton, M. S.; Lillico, A. J.; Fakih, M.; Natarajan, R.; Clark, L. C.; Marshall, J. R. A report of high-dose selenium supplementation: response and toxicities. *J Trace Elem Med Biol*. **18:**69-74; 2004.

# Figure legends

**Figure 1.** Phase contrast photomicrographs depicting the STAV-AB mesothelioma cells with epithelioid morphology (A) and the STAV-FCS mesothelioma cells with sarcomatoid morphology (B) (bar = 50 μm).

**Figure 2.** Effects of selenite and doxorubicin on cell viability. Treatment with doxorubicin shows a dose and time dependent inhibitory effect on epithelioid (A) but not sarcomatoid (B) mesothelioma cells. Asterisks denote a statistically significant difference from the cells treated with the lowest dose (0,2 μg/ml). The dose-response curve for selenite (C) indicates sensitivity of both mesothelioma phenotypes after 28 h, the effects being more pronounced in the sarcomatoid cells. Asterisks denote a statistically significant difference between phenotypes. The response to 7,5 μM of selenite was similar in three other three mesothelioma cell lines (MM) and two adenocarcinoma cell lines (Adeno), while the benign mesothelial cells remained unaffected (D). Asterisks denote a statistically significant difference from both populations of benign mesothelial cells. The combination of selenite and doxorubicin inhibited both epithelioid (E) and sarcomatoid (F) mesothelioma cells. Asterisks denote a statistically significant difference from the untreated control (not shown in the diagram). Error bars show the standard error of the mean (SEM).

**Figure 3.** Selenite induces apoptosis in mesothelioma cells. The morphological examination and FACS analysis of apoptosis correlate. Morphological determination of

apoptosis in relation to concentration of selenite is shown in epithelioid (A) and sarcomatoid cells (B). Asterisks denote a significant difference from untreated cells. The proportion of apoptotic cells, as estimated from pyknotic index, was dose dependent with higher sensitivity to selenite in sarcomatoid (B) cells than in epithelioid ones (A). Apoptosis could also be demonstrated with a similar dose dependence by FACS analysis (C, D). The Y-axis depicts the fluorescence intensity of propidium iodide (PI) and the X-axis the log of fluorescence intensity of Annexin V. Dose and time dependent increase of the apoptotic cells can be observed in both phenotypes (C, D). The epithelioid cell population shows signs of early apoptosis (lower right quadrant) in a substantial proportion of cells only after 52 hours (C), whereas the sarcomatoid cells are apopotic already after 28 hours (D). The cells in the upper right quadrant are late apoptotic and correspond very well to the proportion of pyknotic cells in morphological examination in both the epithelioid (A, C) and sarcomatoid (B, D) phenotypes. As nearly no morphological signs of necrosis were visible, we consider the cells in the upper right quadrant for the most part to be in a later phase of apoptosis.

**Figure 4.** Selenite treatment decreases the thioredoxin reductase 1 (TrxR1) activity (A) and the glutathione peroxidase (GPx) activity (B), in cells of the two mesothelioma phenotypes. The cells were grown for 48 hours in culture medium, and supplemented with different concentrations of selenite for 48 hours.

**Figure 5.** ROS generation by selenite in malignant mesothelioma cells. Representative micrographs showing untreated controls of sarcomatous STAV FCS cells (A), STAV

FCS cells treated with 5 μM selenite (B), untreated controls of epithelioid STAV AB cells (C), and STAV AB cells treated with 5 μM selenite (D). In the STAV FCS cells, selenite generates ROS. The converse effect appears in the STAV AB cells.

**Figure 6.** The toxic effect of 7.5 μM selenite was abrogated by 1 mM ascorbic acid, indicating that the toxicity of selenite is mediated by oxidative stress. Asterisks denote a significant difference between cells treated with selenite and ascorbic acid and cells treated with only selenite. Data from one representative experiment are shown.

**Figure 7.** Representative photomicrographs showing immunocytochemical staining for Trx1 (left column) and TrxR1 (right column) in cells exfoliated into pleural effusions. Malignant mesothelioma (A, B) and adenocarcinoma (C, D) cells demonstrated reactivity to both epitopes, while benign mesothelial cells (E, F) remained negative. Pre-incubation of antibodies with excess amounts of Trx1 (G) or TrxR1 (H) protein completely abolished all binding of antibodies to the tumor cells (bar = 50 μm).

**Figure 8.** Immunohistochemical staining for Trx1 (A, C) and TrxR1 (B, D) *in vivo* in biphasic mesothelioma, demonstrating that the enzyme is present in native tumor tissue. The biphasic mesothelioma tissue specimen show marked reactivity to Trx1 and TrxR1 in the epithelial tumor component while the spindle shaped sarcomatoid tumor components remained largely unstained (bar = 50 μm). The images are representative for 9 sampled tumor specimens.

**Figure 9.** Hypothetical model for the cytotoxic effects of selenium. The metabolic product selenide ($HSe^-$) will redox cycle with thiols (R-SH) to generate massive non-stoichiometric amounts of reactive oxygen species (ROS). The redox cycling is increased by free thiols and consumes NADPH. The formation of ROS will cause oxidative stress that damages the cell and is a direct cause for apoptosis. It will also oxidize thiols (R-SH) into disulfides (R-SS-R), thereby creating new covalent bonds within and between proteins. The tertiary structure of the affected proteins will change and they may be unable to maintain their function. Thioredoxin 1 (Trx1) reduces disulfides back into thiol groups in a redox cycle that is catalyzed by TrxR1 and consumes NADPH. Apoptosis Signal Regulating Kinase 1 (ASK-1) is a regulatory protein, which is inactive when bound to reduced Trx1. A shift towards oxidized Trx1 will lead to the release and activation of ASK-1.

**Figure 1**

Click here to download high resolution image

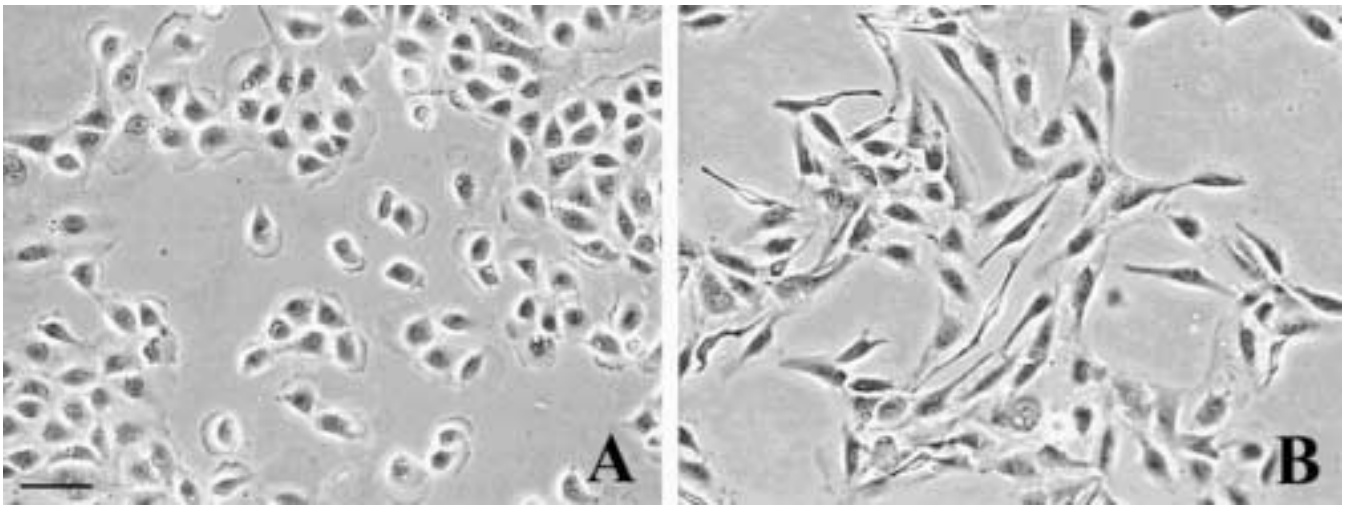

Figure 2-4

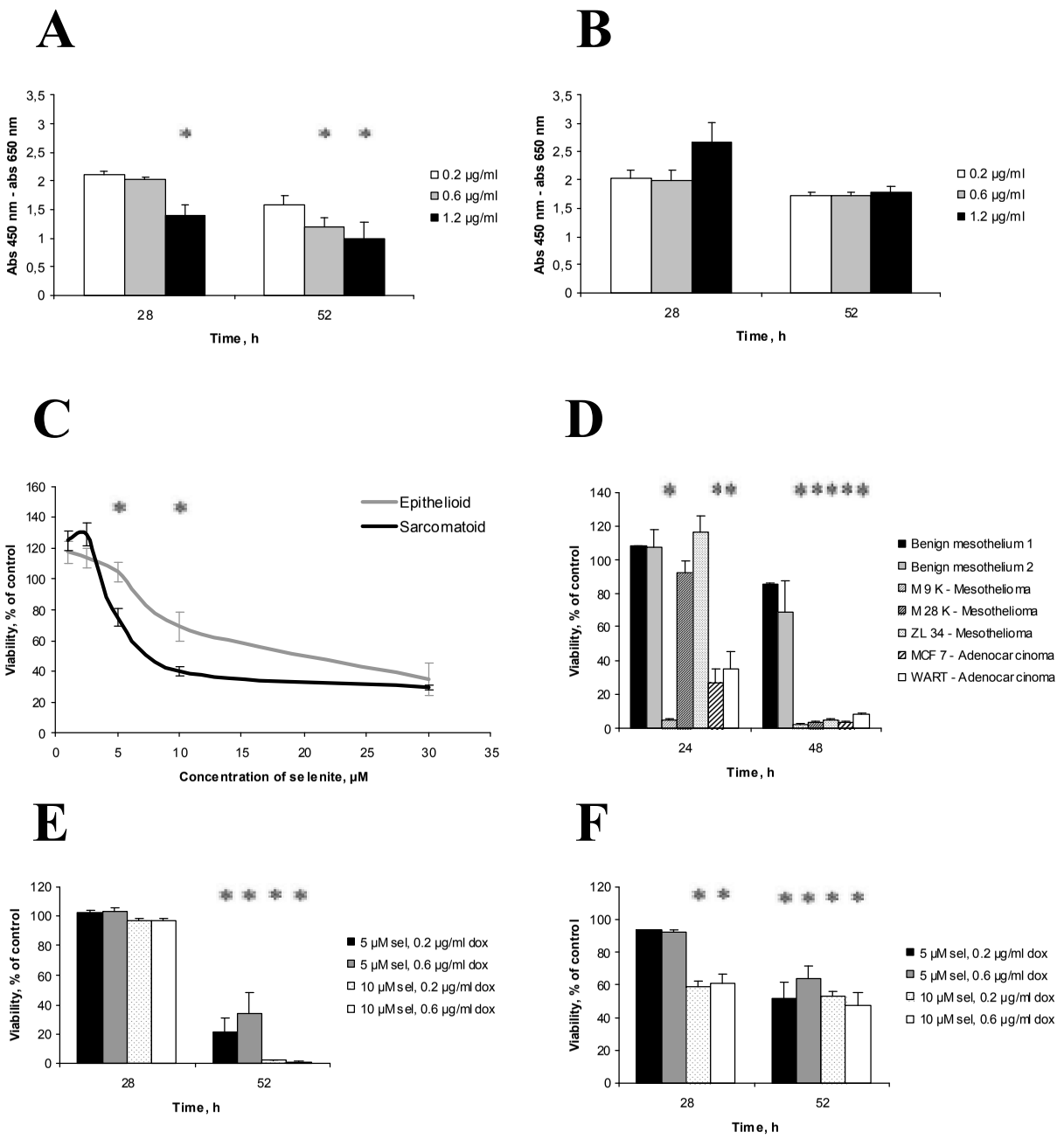


**Figure 2.**

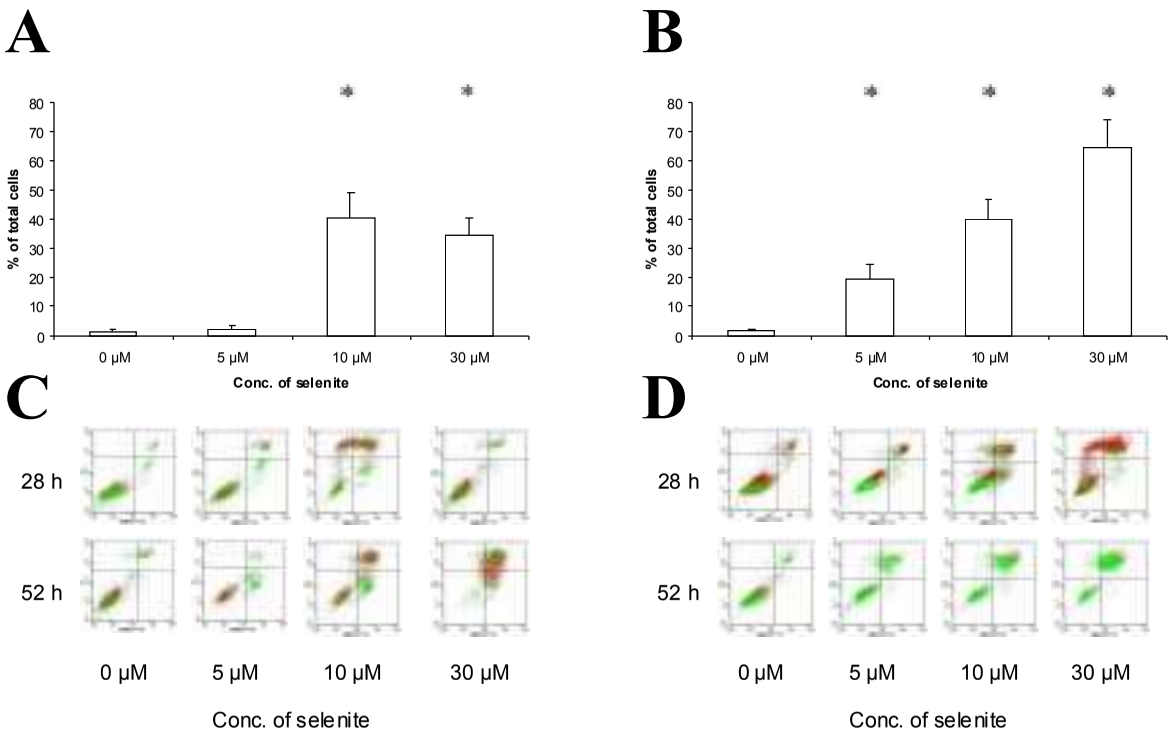
A
B
% of total cells
0 μM
5 μM
10 μM
30 μM
Conc. of selenite
C
D
28 h
52 h
0 μM
5 μM
10 μM
30 μM
Conc. of selenite

**Figure 3.**

**A**

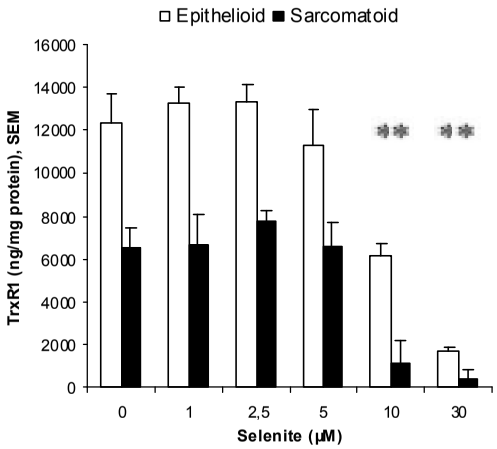
Epithelioid
Sarcomatoid
TrxR1 (ng/mg protein), SEM
16000
14000
12000
10000
8000
6000
4000
2000
0
0
1
2,5
5
10
30
Selenite (µM)

**B**

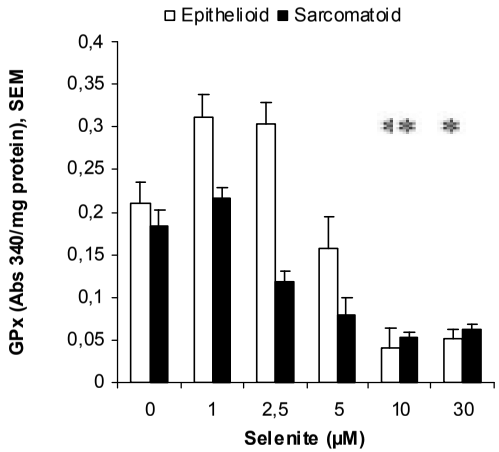
Epithelioid
Sarcomatoid
GPx (Abs 340/mg protein), SEM
0,4
0,35
0,3
0,25
0,2
0,15
0,1
0,05
0
0
1
2,5
5
10
30
Selenite (µM)

**Figure 4.**

**Figure 5**

Click here to download high resolution image

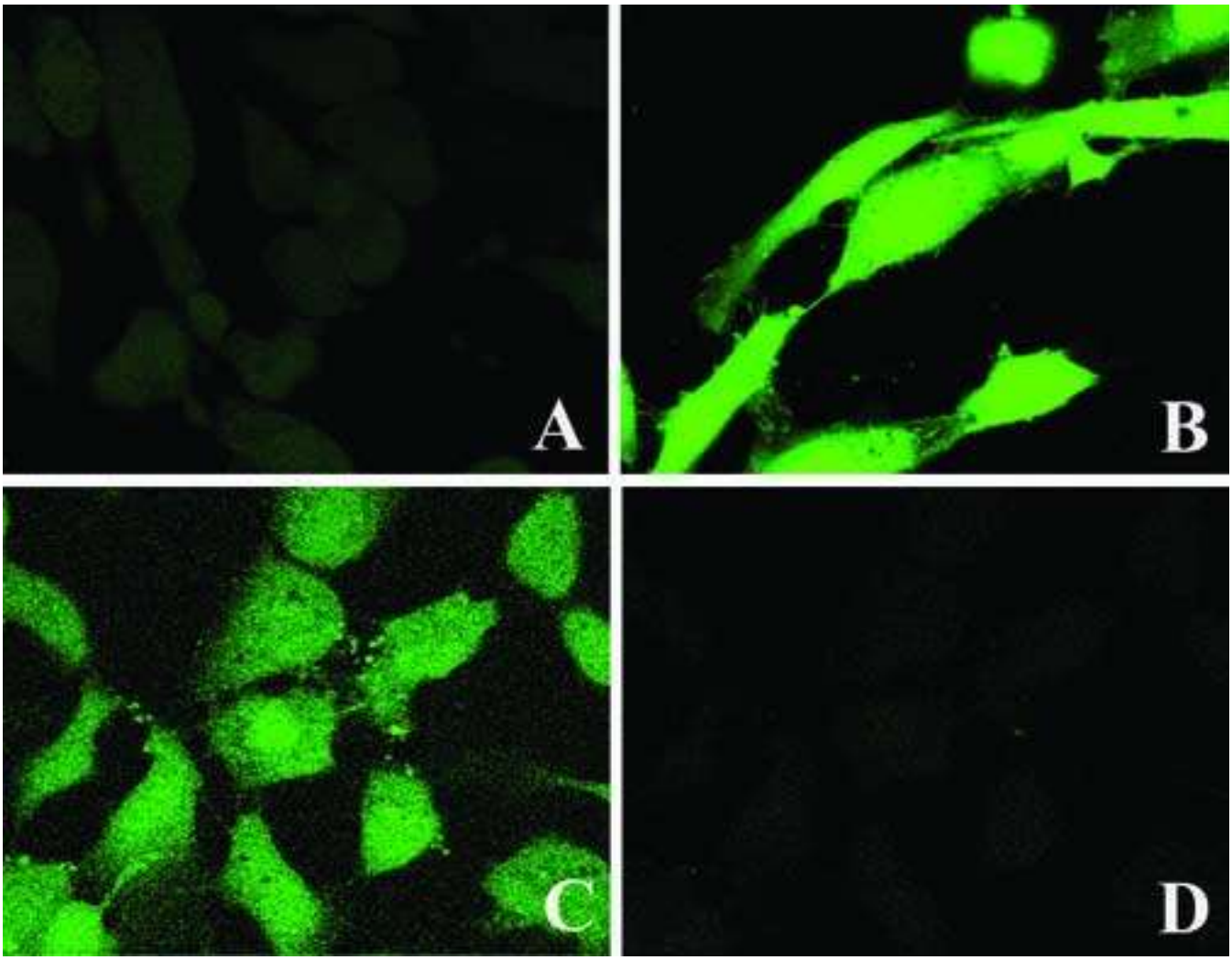

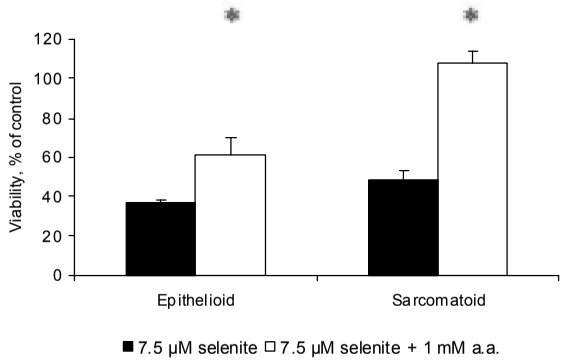
120
100
80
60
40
20
0
Viability, % of control
Epithelioid
Sarcomatoid
7.5 µM selenite
7.5 µM selenite + 1 mM a.a.

# Figure 6.

**Figure 7**

Click here to download high resolution image

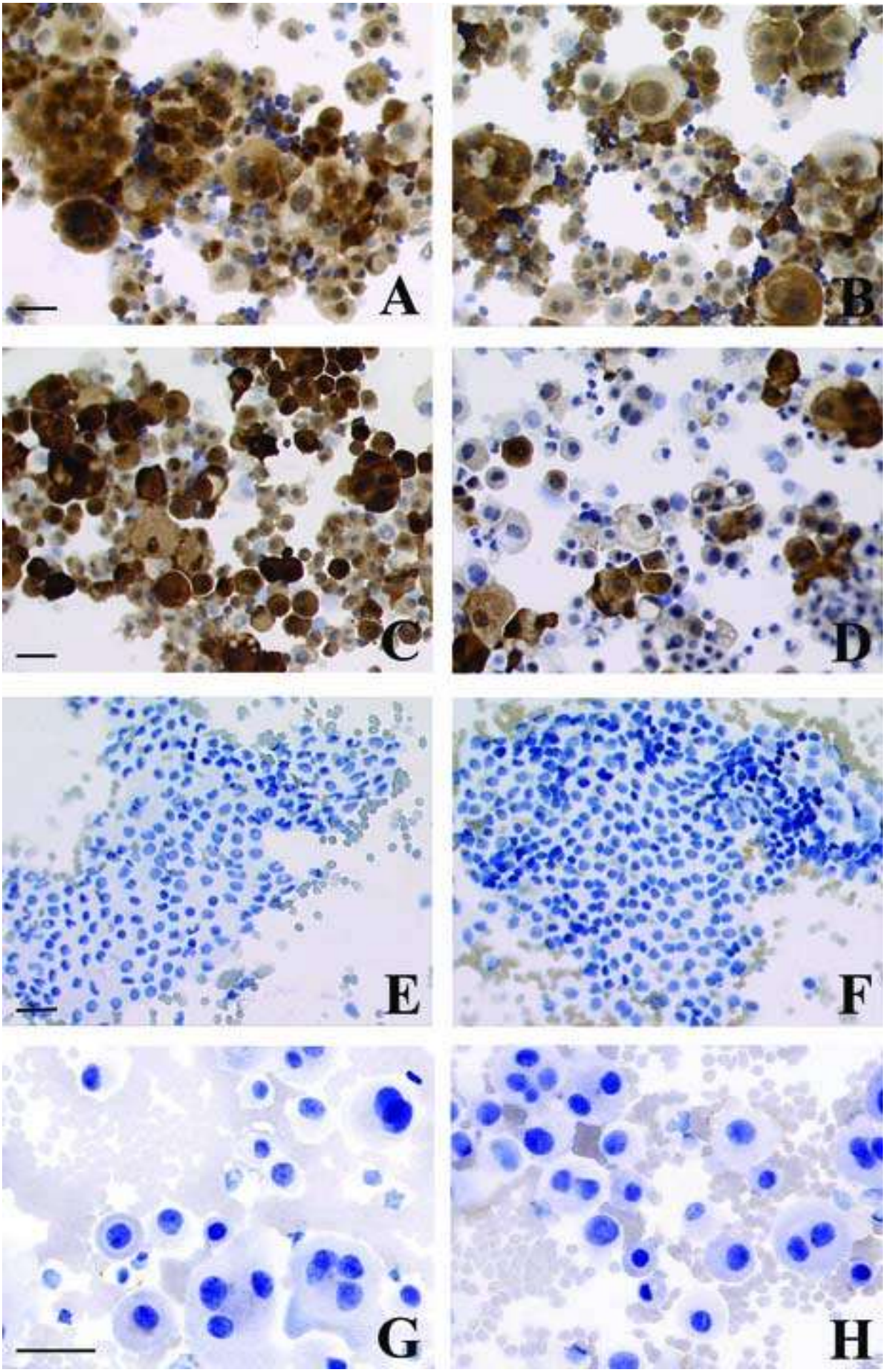

**Figure 8**

**Click here to download high resolution image**

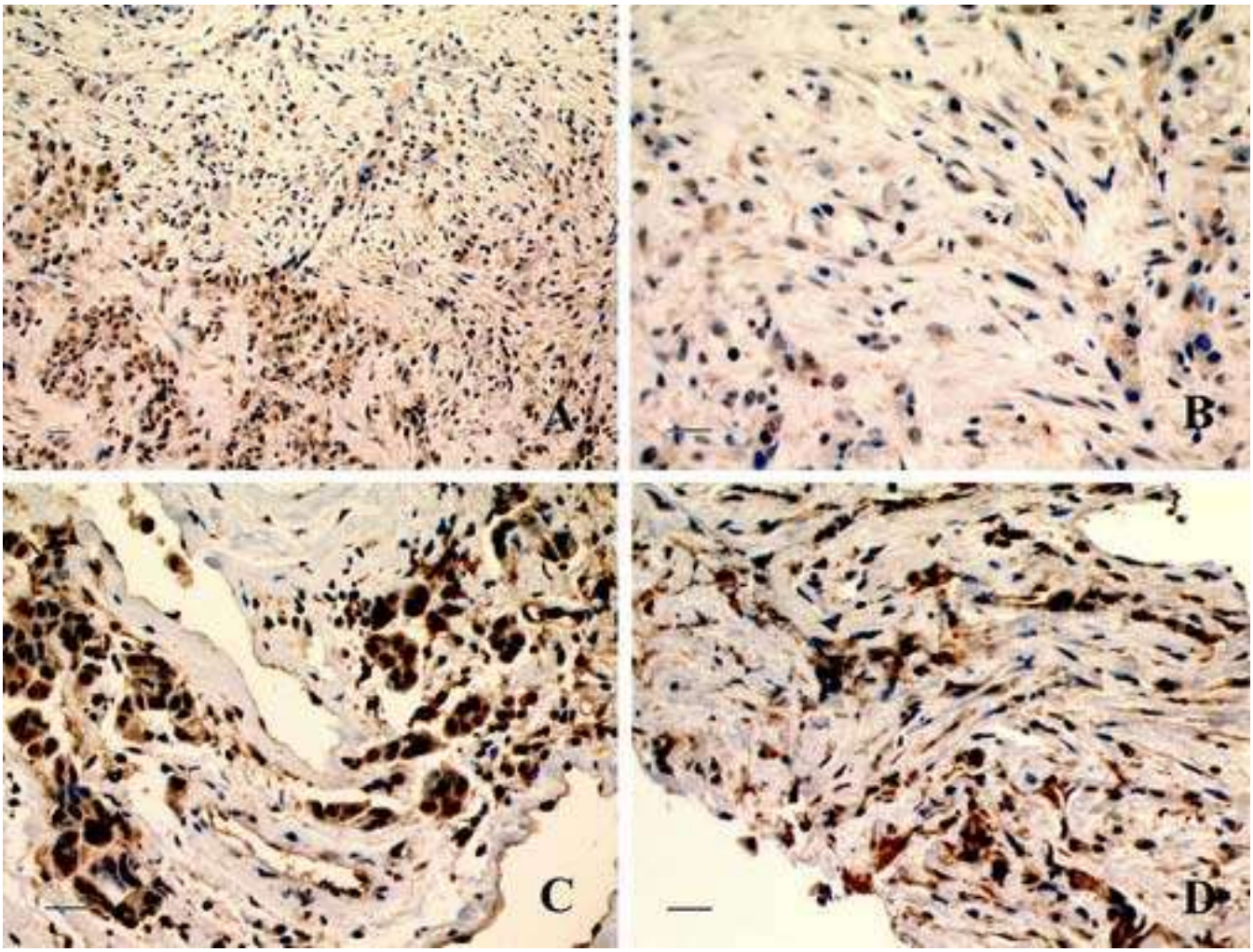

**Figure 9**

**Click here to download high resolution image**